

Effect of particle size on the mechanical properties of reaction bonded boron carbide ceramics

Prasenjit Barick*, Dulal Chandra Jana, Natarajan Thiagarajan

Centre for Non-Oxide Ceramics, International Advanced Research Centre for Powder Metallurgy & New Materials, PO: Balapur, RCI Road, Hyderabad 500005 Andhra Pradesh, India

Received 9 March 2012; received in revised form 22 June 2012; accepted 28 June 2012
Available online 6 July 2012

Abstract

In the present communication, effect of boron carbide particle size on the mechanical properties such as hardness, fracture toughness and flexural strength of reaction bonded boron carbide (RBBC) ceramics were investigated. RBBC composites were produced by the reactive infiltration of molten silicon into porous preform containing boron carbide and free carbon. Boron carbide powders with mean particle size of 18.65 μm , 33.70 μm and 63.35 μm were chosen for the RBBC composites. The experimental results show that hardness increases from $1261.70 \pm 64.74 \text{ kg/mm}^2$ to $1674.90 \pm 100.00 \text{ kg/mm}^2$ and fracture toughness drops from $5.76 \pm 0.26 \text{ MPa m}^{1/2}$ to $3.4 \pm 0.37 \text{ MPa m}^{1/2}$. However, flexural strength decreases from $403.41 \pm 5.70 \text{ MPa}$ to $256.15 \pm 25.05 \text{ MPa}$ with the increase in particle size. Indentation induced cracks in RBBC are mainly median type and number of cracks increase with the increase of starting particle size.

© 2012 Elsevier Ltd and Techna Group S.r.l. All rights reserved.

Keywords: C. Mechanical properties; RBBC; Particle size

1. Introduction

Reaction bonded boron carbide (RBBC) is an alternative for hot-pressed monolithic boron carbide. In the fabrication of RBBC, a porous preform (porosity 20–25%) containing boron carbide and/or free carbon is infiltrated with molten silicon at 1450–1600 °C under vacuum (typically 10^{-3} – 10^{-4} Torr) [1–3]. Molten silicon infiltrates into the porous preform and spontaneously reacts with free carbon and forms silicon carbide. This silicon carbide occupies a fraction of the total pores and remaining pores in the preform are filled with silicon. The reaction formed silicon carbide, residual Silicon, and pre-existing boron carbide particles are interconnected into a uniform and strong three dimensional network [3]. It is also reported that a ternary boron carbide based compound $\text{B}_{12}(\text{B,C,Si})_3$ is found at the peripheral region of boron carbide particles [3,4].

The novelty of reaction bonding technique lies in its low processing temperature (1450 °C–1600 °C) and ability to

produce near net shape product with zero shrinkage [5,6]. These processing advantages combined with low mass to volume ratio (2.57 gm/cm^3) and excellent mechanical property, e.g. hardness ($\text{HV}_2 = 2807 \pm 54 \text{ kg/mm}^2$), flexural strength ($278 \pm 14 \text{ MPa}$), and Young's modulus ($382 \pm 6 \text{ GPa}$) of RBBC make it a potential material for ballistic application [5]. The high hardness value ($2807 \pm 54 \text{ kg/mm}^2$) of RBBC is attributed to the presence of high hardness monolithic boron carbide [5]. In RBBC, hardness depends upon the relative amount of phases present e.g. boron carbide, silicon carbide, and silicon in the microstructure.

Mechanical property of polycrystalline material depends upon several parameters like grain size and their distribution, porosity, pore size distribution, inclusions, agglomerations, and impurities in the starting materials [7]. Presence of flaws in the form of microcracks and pores reduce real fracture strength of ceramics at least by two orders of magnitude than the theoretical value [7–9]. The cracks which nucleate at grain boundary of polycrystalline ceramics may propagate up to one grain diameter [7]. Ceramics with smaller grain size exhibits higher fracture strength according to Griffith equation $\sigma_f = (2\gamma Y/\pi C)^{1/2}$

*Corresponding author. Tel.: +91 40 24457104; fax: +91 40 24442699.
E-mail address: pbarick@yahoo.com (P. Barick).

where ' σ_f ' is the fracture strength in MPa, ' γ ' is the fracture surface energy (J/m^2), ' C ' is half of the crack length (μm) and ' Y ' is the Young's modulus in GPa [8]. Therefore, grain size has an important implication in controlling the mechanical property of engineering materials. Hence, it is important to address the mechanical property—particle size issue for such an important material like RBBC in order to construct a preliminary platform towards tailoring its properties.

Various aspects of reaction bonded boron carbide have been studied by several researchers. Hayun et al. [4] have shown that a suitable particle size distribution in starting powder mixture improves the mechanical properties of RBBC composite significantly. With the use of suitable particle size distribution, it was possible to increase the density of green preform to 75% of theoretical density. Free silicon content eventually reduced to 8–10 vol% in RBBC composite, which enhance hardness ($\text{HV}_{2000\text{g}} = 2300 \pm 250 \text{ kg/mm}^2$), flexural strength ($318 \pm 20 \text{ MPa}$) and Young's modulus ($400 \pm 10 \text{ GPa}$). Use of particle size distribution plays a crucial role to reduce free silicon content in RBBC and to improve mechanical properties. Another study shows that, RBBC microstructure consists of polygon shaped SiC, if boron carbide powder blend was prepared with free carbon [3]. Plate shaped silicon carbide was observed while starting composition for RBBC was made without free carbon [3]. A recent report shows that dissolution–precipitation mechanism is the possible cause for the formation of $\text{B}_{12}(\text{B,C,Si})_3$ at the outer region of boron carbide grains in RBBC, which is called as core–rim structure [3,10]. Chhilar et al. [11] have shown that the increase of residual silicon in RBBC decreases its hardness, flexural strength and Young's modulus but increases fracture toughness. Presence of residual silicon in RBBC matrix can increase the fracture toughness value to $5 \text{ MPa m}^{1/2}$ comparing with that of monolithic boron carbide ($\approx 3 \text{ MPa m}^{1/2}$) [12].

In this study, we have investigated the influence of boron carbide particle size on mechanical properties such as hardness, fracture toughness, indentation induced crack propagation behavior and flexural strength of RBBC ceramics.

2. Experimental procedure

2.1. Powder processing

Commercial grade boron carbide powders of mean particle size $D_{50} = 18.65 \mu\text{m}$, $D_{50} = 33.70 \mu\text{m}$, and $D_{50} = 63.35 \mu\text{m}$ [Speedfam India (Pvt.) Limited, India] and carbon black (Phillips Carbon Black Limited, India) were used as starting raw materials. The particle size distribution of boron carbide powders, measured by granulometer (CILAS920, France) is presented in Table 1. For the ease of identification, the powders are designated as RB-1, RB-2 and RB-3. The morphology of boron carbide powders in Fig. 1(a–c) shows that the powders are free from agglomerates and particle shape is irregular with sharp edges and corners. The powder

Table 1

Particle size distributions of boron carbide powders.

Powder	Particle size distribution*		
	$D_{10} (\mu\text{m})$	$D_{50} (\mu\text{m})$	$D_{90} (\mu\text{m})$
RB-1	7.47	18.65	45.48
RB-2	21.63	33.70	53.07
RB-3	37.48	63.35	187.47

*Measured by 'CILAS920 granulometer'.

mixture was prepared with 87.20 wt% boron carbide, 2.44 wt% carbon black and 10.37 wt% phenolic resin (estimated carbon content of resin was 36.04 wt%). Resin served as an organic binder and a source of carbon. The net amount of carbon (7 vol%) has come from direct addition of carbon black and through pyrolyzation of above-mentioned resin. For each type of powder (RB-1, RB-2, and RB-3), a batch of 100 g powder was prepared by ball milling of boron carbide and carbon black in acetone medium using ZrO_2 balls. Resin was added 2 h prior to the completion of milling. Finally, acetone was removed from resultant slurry to obtain a dry powder mass. These powders were screened through a 60 BSS sieve to avoid the presence of agglomerates. Premix powder was uniaxially compacted at 140 MPa using a metallic die to obtain green specimens.

2.2. Binder removal and silicon infiltration

All the green preforms were slowly heated (1°C/min) to 550°C with dwell time of 60 min in order to burn out resinous binder. Subsequently, infiltration was carried out with molten silicon in a resistance heating graphite furnace under vacuum (65×10^{-6} Torr) at 1550°C for 30 min.

2.3. Characterization technique

Relative density of green preforms was measured and is presented in Table 2. Phase evaluation of the composites were performed by a powder X-ray diffractometer (D8 Advanced system, BRUCKER, axs, Germany) using $\text{Cu-K}\alpha$ as characteristics radiation of wavelength $\lambda = 1.54187 \text{ \AA}$. Microstructures of the polished specimens (optical finish with $1 \mu\text{m}$ diamond slurry) were examined using scanning electron microscopy (S-3400N, HITACHI, Japan) operated at 20 KV. Image analysis for scanning electron micrographs was conducted using ANALYSIS 5 software (Olympus, USA) to evaluate the ratio of average grain size to silicon thickness in RBBC composites. Hardness was determined using a microhardness tester (UHL VMHT, Wateruhl technische Mikroskopie GmbH & Co. KG, Germany) with a Knoop indenter under 9.80 N load. Vickers indenter was used at 9.80 N load to generate cracks on the sample surface using same hardness tester. Fracture toughness of test bars ($45 \text{ mm} \times 4 \text{ mm} \times 3 \text{ mm}$) was measured using the single edge notch beam (SENB) technique with a notch width of $300 \mu\text{m}$, a span of 40 mm and a cross-head

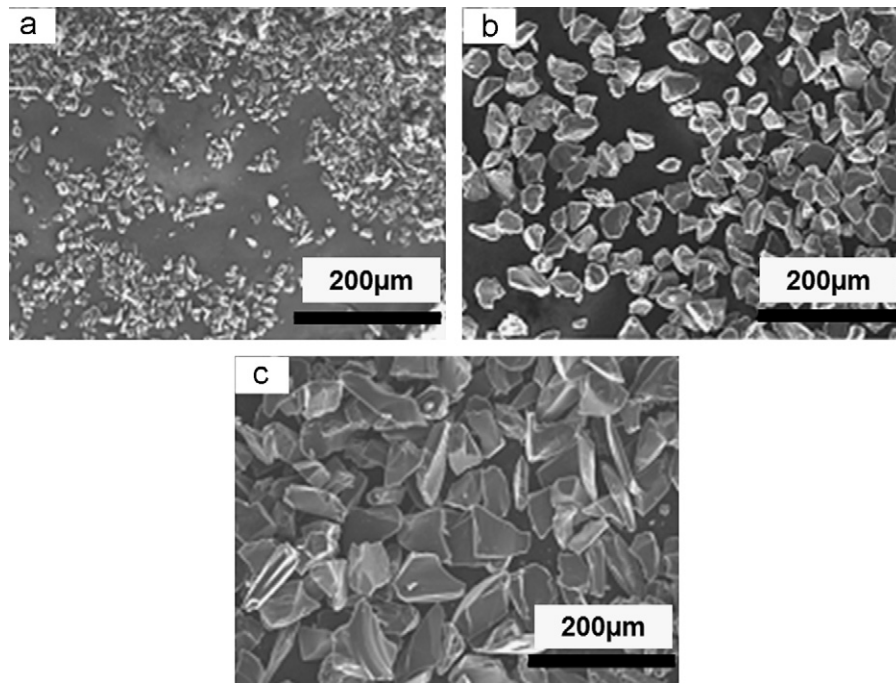


Fig. 1. Scanning electron micrographs of boron carbide powders: (a) $D_{50}=18.65\ \mu\text{m}$ (RB-1); (b) $D_{50}=33.70\ \mu\text{m}$ (RB-2); and (c) $D_{50}=63.35\ \mu\text{m}$ (RB-3).

Table 2
Relative density of green preforms.

Sample	Relative density of green preforms (%)
RB-1	55.89
RB-2	58.94
RB-3	62.67

speed of 0.5 mm/min. Flexural strength of test specimens ($21\ \text{mm} \times 4\ \text{mm} \times 3\ \text{mm}$) was carried out following three point bending mode in a universal testing machine (INSTRON-4483) using a span of 16 mm with crosshead speed of 0.5 mm/min.

3. Results and discussion

3.1. XRD observations

X-ray diffraction patterns (Fig. 2) of RBBC composite samples were analyzed with reference to ICDD PDF-4+2009 RDB database. Phases present in RBBC microstructure, were identified using Rietvelt analysis. The identified phases were $\text{B}_{12.94}\text{C}_2$ (ICDD card no. 04-007-9814), $\text{B}_{13.72}\text{C}_{1.52}$ (ICDD card no. 04-009-6158), SiC (β -form) (ICDD card no. 04-008-1657), Si (ICDD card no. 04-012-7888), $\text{CaAl}_2\text{Si}_2\text{O}_8$ (ICDD card no. 04-011-5378), FeSiO_3 (ICDD card no. 04-009-1850), ZrO_2 (04-010-3279) and ICDS database (card no. 00-019-0178) was used for identification of B_4C .

As expected, silicon carbide formed due to the reaction between carbon and molten silicon. It is reported in

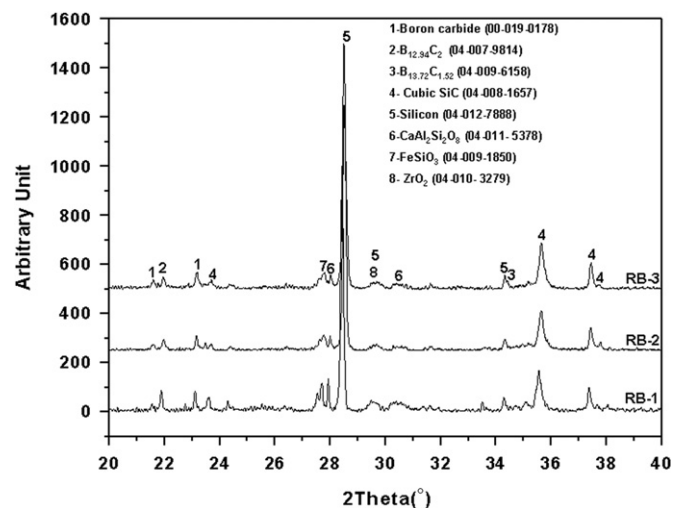


Fig. 2. X-ray diffraction pattern of reaction bonded boron carbide composites with different particle sizes.

literature that, SiC also formed due to the reaction between boron carbide and molten silicon as $\text{Si(l)} + 3\text{B}_4\text{C(s)} = \text{SiC(s)} + \text{B}_{12}(\text{B,C, Si})_3(\text{s})$ [13,14]. However, it was difficult to differentiate between SiC formed due to the above mentioned two mechanisms. Presence of calcium aluminosilicate and iron silicate in XRD pattern were due to the reaction between trace impurities (Ca, Fe) present in boron carbide powder with molten silicon. This relative increase of peak intensity for RB-1 may be due to strong polycrystalline nature of $\text{CaAl}_2\text{Si}_2\text{O}_8$ and FeSiO_3 because of high potential towards their formation for smaller particle size or may be due to preferential orientation. However, it needs further investigations to find the exact

cause. The presence of ZrO_2 was due to contamination from the milling media.

3.2. Microstructural analysis

3.2.1. Scanning electron microscopic analysis

Fig. 3 (a–c) shows the back scattered scanning electron micrographs for three RBBC composites made from aforementioned different particle sizes. SEM images revealed that boron carbide particles (dark gray) are uniformly distributed and interconnected with reaction formed silicon carbide (light gray) and silicon (white) phases. This color contrast appears due to variation in atomic number of each phase present in the microstructure. It is observed from SEM that RBBC composites are free of pore or void. Total amount of pores in the composite is partially occupied by in-situ reaction formed silicon carbide and remaining pores got filled with residual silicon because conversion of carbon to silicon carbide due to reaction with molten silicon is associated with 2.33 times volume expansion [15].

3.3. Mechanical properties

3.3.1. Hardness and fracture toughness

Fig. 4 shows the hardness and fracture toughness of reaction bonded boron carbide composites as a function of particle size. Average hardness values calculated from ten numbers of indentations are represented with error bars in Fig. 4. The hardness value of RBBC composites increases from $1261.70 \pm 64.74 \text{ kg/mm}^2$ to $1674.90 \pm 100.00 \text{ kg/mm}^2$ and fracture toughness decreases from 5.76 ± 0.26 to

$3.4 \pm 0.37 \text{ MPa m}^{1/2}$ with the increase in boron carbide starting particle size from $18.65 \mu\text{m}$ to $63.35 \mu\text{m}$. This increasing trend of hardness can be expressed as $Y=1079.35+9.33X$ while decreasing trend of fracture toughness can be represented as $Y=6.74-0.05X$, where 'X' axes represents starting particle size and 'Y' axis represents hardness and fracture toughness in Fig. 4. In polycrystalline material, hardness decreases when smaller size grains transform to larger size because of decrease in grain boundary area. Precipitation hardened material with uniformly dispersed fine particles exhibits higher strength. When these dispersed fine particles coalesce with each

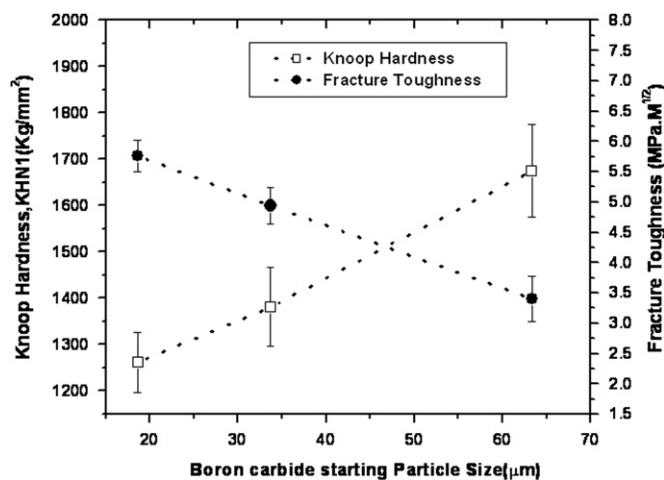


Fig. 4. Hardness and fracture toughness of RBBC composites as a function of boron carbide starting particle size.

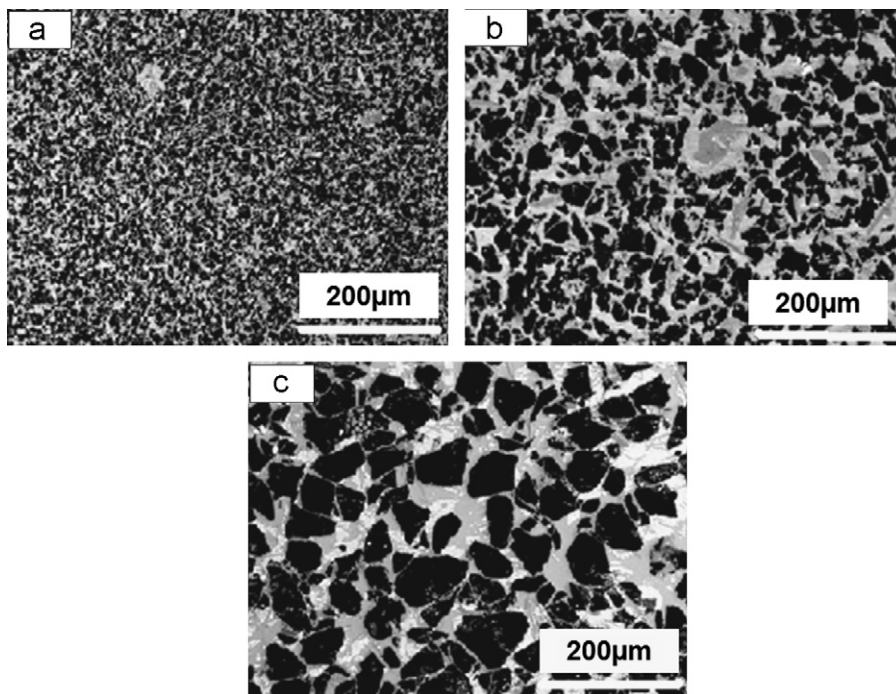


Fig. 3. Scanning electron micrographs of polished surface of (a) RB-1, (b) RB-2, and (c) RB-3 composites (dark gray color—boron carbide, light gray color—SiC, white color—silicon).

other and form larger size particles, the strength drops as the interparticle spacing increases because strength or hardness and interparticle spacing are inversely proportional to each other.

Reaction bonded boron carbide is a multiphase ceramic containing boron carbide, silicon carbide and silicon. Here, no grain growth mechanism is present. The particle size dependent hardness phenomenon may not be explained using the above said concept for RBBC ceramics.

For the composite RB-1, fine boron carbide grains are uniformly distributed in the microstructure. Fineness of powder increases the surface area. Therefore, RBBC composite with fine grain size consist maximum boundary area in comparison with larger size particles [16]. Interface boundary is generally a weak zone. During hardness measurement, the amount of weak interfacial area under the indenter is expected to be more for RBBC composite with smaller size starting particles (i.e. RB-1). As a result, RB-1 shows minimum hardness as its indentation size is larger at a given load. Accordingly, RB-2 and RB-3 composites show medium and maximum hardness value.

K_{IC} or fracture toughness is directly proportional to strain energy released per unit area of crack surface, developed during the propagation of unstable crack [7,8]. To release more energy, the fracture path must be longer. A crack during propagation will go around the grains. The number of grains for crack propagation that will pass through depends upon the average grain size and intergranular silicon thickness [17]. The ratio of average grain size and silicon thicknesses are 3.36, 3.08 and 2.71 for RB-1, RB-2 and RB-3 composites respectively, as estimated through image analysis. Accordingly, a crack will propagate longest distance

for RB-1 type composite and smallest distance for RB-3 and medium distance for RB-2 for a given volume fraction of composite. Thus, K_{IC} will be maximum for RB-1 and minimum for RB-3. This type of phenomenon in reaction bonded silicon carbide ceramics has also been observed in the work reported by Chakrabarti et al. [17].

Further, RBBC composite possibly fails due to three types of fracture mechanisms namely, (i) fracture in boron carbide grains i.e. transgranular fracture, (ii) failure due to interfacial debonding from free silicon and (iii) deformation in silicon. Among all the mechanisms, silicon deformation has major contribution towards substantial improvement of fracture toughness ($\approx 5 \text{ MPa m}^{1/2}$) for reaction bonded boron carbide ceramics. The fracture toughness for pristine boron carbide or hot pressed boron carbide is $2.9\text{--}3.7 \text{ MPa m}^{1/2}$ [18]. Residual silicon or free silicon in RBBC ceramics, fractured in semi-ductile mode during failure, causes higher K_{IC} [12,19]. As the particle size or grain size decreases, interfacial debonding mechanism dominates over transgranular fracture [19]. Debonding at boron carbide–silicon and silicon carbide–silicon interface has more contribution towards the enhancement of fracture toughness as compared to transgranular failure mode [20]. This led to highest fracture toughness for RB-1, medium for RB-2 and lowest fracture toughness for RB-3. Moreover, it is realized from SEM fractographs of the composites (Fig. 5(a–c)) that degree of smoothness for fracture surface increases with increased particle sizes. Maximum extent of non-planarity is observed at fracture path of RB-1, medium for RB-2 and lowest for RB-3, and concurrently same type of behavior is observed in the deformation of silicon. As a result, RB-1 with smallest particle size exhibits highest fracture toughness

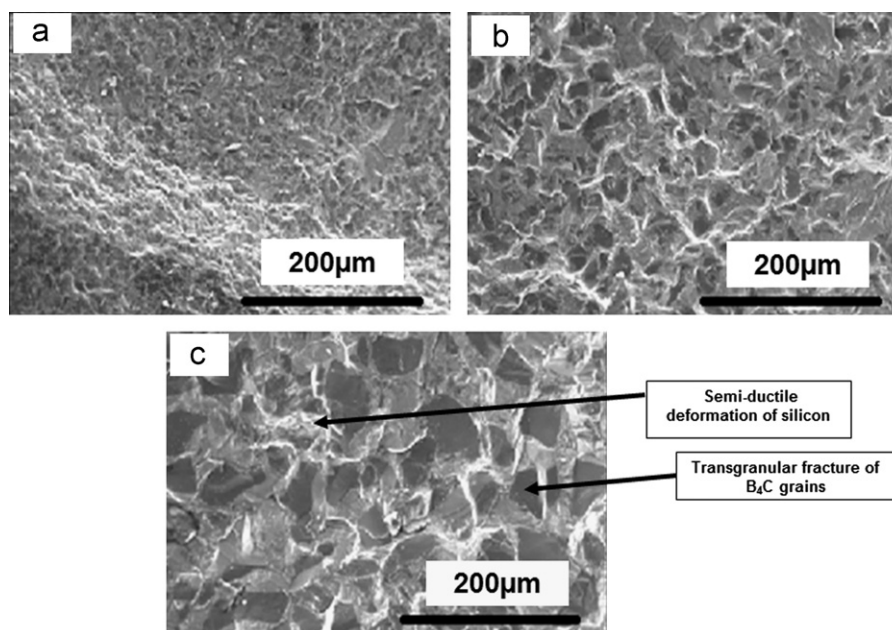


Fig. 5. Scanning electron micrographs of the fracture surface of (a) RB-1, (b) RB-2, and (c) RB-3. Dark gray color—boron carbide and white color—silicon.

and RB-3 shows least fracture toughness, while, RB-2 demonstrates intermediate fracture toughness.

3.3.2. Indentation induced crack propagation behavior

It is known that the presence of cracks in the material alters its state of stress because significant energy is required for the propagation of nucleated cracks, compared to the energy that is essential to produce plastic yield. In polycrystalline, brittle materials, such cracks can be generated and propagated by the application of sharp indenters like Vickers and Knoop. Accordingly, RB-1, RB-2 and RB-3 samples have been subjected to the Vickers indentation technique for the development of indentation induced cracks. It is intended to study the qualitative mechanical behavior of these samples based on their cracking pattern, crack path and crack type. The experimental quantitative data is useful to make a comparative statement among composites with different particle sizes, which provides the indication about material's behavior under indentation load.

Vickers microhardness tester has been used to introduce cracks on all the reaction bonded boron carbide composite samples. No appreciable crack was observed at loads of 1.96 N and 4.90 N.

In all the indentations made on RB-1, RB-2 and RB-3 samples, mostly median cracks (at the tip of the impression) nucleate at the interface region between plastically and elastically deformed materials observed with different lengths. Occasional formation of lateral cracks has also been noticed in some cases. These cracks were of varying widths ranging from $0.3\ \mu\text{m}$ to $0.7\ \mu\text{m}$ in all the samples. In most of the cases, cracks traveled across the boron carbide grains and

terminated at the softer 'Si' zone. Sometimes cracks traveled 2–3 grains of boron carbide in addition to traveling through the softer silicon region. This indentation induced crack path and their patterns are shown in Fig. 6(a–c). Since, boron carbide has strong covalent bonding and grain boundary cohesive force, it is expected that the transgranular type of cracking path occurs in all the samples. Further, relationship between fracture toughness and average number of cracks with the boron carbide particle size is shown in Fig. 7. With the increasing boron carbide particle size, there is an increase in the number of average cracks which reflect the declining trend of fracture toughness with grain size.

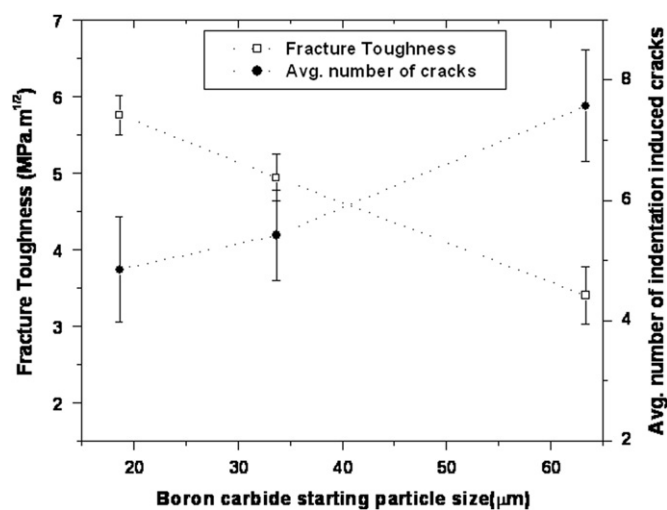


Fig. 7. Fracture toughness and average number of indentation induced cracks as a function of boron carbide starting particle size.

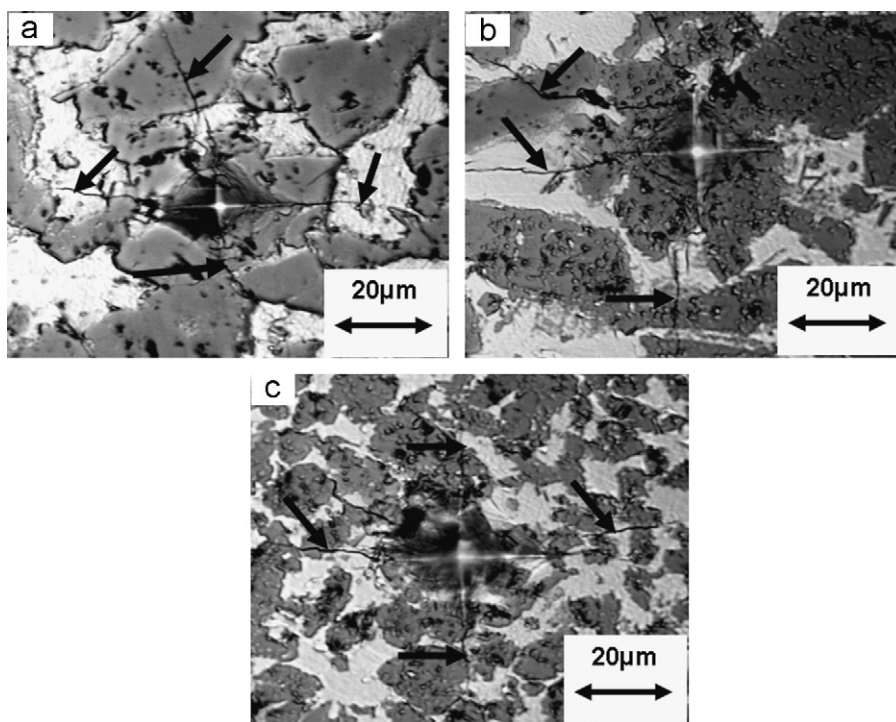


Fig. 6. Optical micrographs of Vickers indentation imprints for (a) RB-1, (b) RB-2 and (c) RB-3 composites. Arrow marks indicate indentation induced cracks.

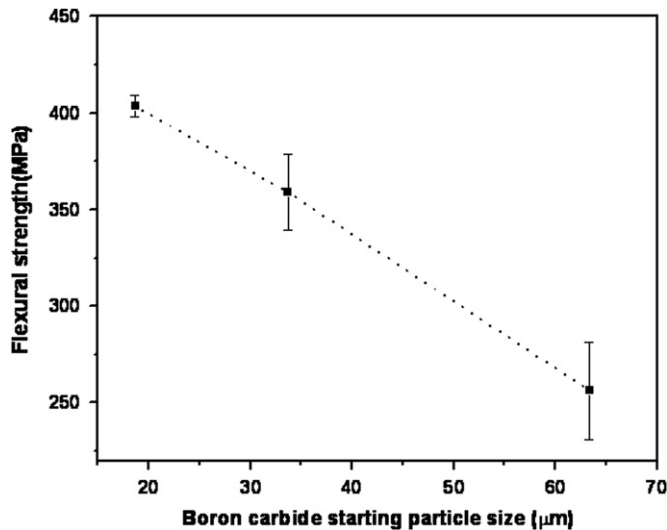


Fig. 8. Flexural strength of RBBC composites as a function of boron carbide starting particle size.

3.3.3. Flexural strength

The room temperature flexural strength as a function of boron carbide starting particle size for RBBC composites is shown in Fig. 8. Flexural strength drops from 403.41 ± 5.70 to 256.15 ± 25.05 MPa while boron carbide particle size increases from $18.65 \mu\text{m}$ to $63.35 \mu\text{m}$. A mathematical equation $Y = 464.05 - 3.25X$ is generated to express the decreasing trend for particle size dependent flexural strength of RBBC ceramics, where 'X' axis represents particle size and 'Y' axis represents flexural strength. Average flexural strength data along with error bars are presented here.

In RBBC, residual stress develops during cooling at weak interfacial sites because of thermal expansion mismatch between boron carbide (CTE: $5.73 \times 10^{-6}/\text{K}$) [18], and silicon (CTE: $3.07 \times 10^{-6}/\text{K}$) [8]. This thermal stress further generates cracks or flaws at interfacial areas. The mean particle size (D_{50}) for RB-3 composite is the largest one ($63.35 \mu\text{m}$). Hence, the probability of largest flaw size formation is highest for RB-3 composite because the scale of interfacial zone between boron carbide grains and silicon is maximum [7]. In addition, flaws generated at the interface, propagate maximum up to one grain size [7]. Therefore, RB-3 with largest boron carbide grains should consist of largest flaws among all the composites. As a result, composite with smallest particle size, i.e. RB-1 exhibits highest flexural strength and RB-3 shows least flexural strength as Griffith equation describes that fracture strength is inversely proportional to the square root of crack length, whereas RB-2 shows an intermediate value which is consistent with other mechanical properties [21].

4. Conclusions

In this study, an investigation was carried out to study the effect of starting boron carbide particle size on the mechanical properties including hardness, fracture toughness and

flexural strength of reaction bonded boron carbide ceramics. The observations are summarized below:

- Hardness of RBBC composite increases with the increase of starting particle size, because of decrease in the volume fraction of weak interfacial area.
- There is a decreasing trend in fracture toughness with the increase of boron carbide starting particle size. This phenomenon is in agreement with the facts that (i) decrease in the ratio of boron carbide grain size and silicon thickness in RBBC composites; (ii) domination of transgranular fracture mechanism over interfacial debonding mechanism; and (iii) lesser degree in non-planarity at fracture path with the increase in particle size.
- Indentation induced cracks in RBBC are median type.
- Flexural strength decreases with the increase in starting particle size due to larger size flaw formation in RBBC, containing larger boron carbide grains.

Acknowledgment

The authors thank Dr. S.N. Dikshit, Technical Advisor (Armor Ceramics), ARCI, Hyderabad, for his valuable suggestions during this study.

References

- M.K. Aghajanian, B.N. Morgan, J.R. Singh, J. Mears, R.A. Wolffe, A new family of reaction bonded ceramics for armor applications, Ceramic Armor Materials by Design Ceramic Transactions 134 (2006) 527–540.
- K.M. Taylor, R.J. Pallick, Dense carbide composite for armor and abrasives. *USP*, 3,765,300...16(1973).
- S. Hayun, N. Frage, M.P. Dariel, The morphology of ceramic phases in B_4C -SiC-Si infiltrated composites, *Journal of Solid State Chemistry* 179 (2006) 2875–2879.
- S. Hayun, A. Weizmann, M.P. Dariel, N. Frage, The effect of particle size distribution on the microstructure and mechanical properties of boron carbide-based reaction bonded composites, *International Journal of Applied Ceramic Technology* 6 (2008) 492–500.
- M.K. Aghajanian, A.L. McCormick, B.N. Morgan, A.F. Liszkiewicz Jr., Boron carbide composite bodies, and methods for making same, *USP* 7332221 B2 19 (2008).
- M. Wilhelm, M. Kornfeld, W. Wruss, Development of SiC-Si composites with fine grained SiC microstructures, *Journal of the European Ceramic Society* 19 (1999) 2155–2163.
- M.W. Barsoum, *Fundamentals of Ceramics*, The McGraw-Hill Companies Inc., NY, USA, 1997.
- V. Raghavan, *Materials Science & Engineering*, Prentice-Hall of India, New Delhi, India, 2000.
- D.J. Green, *An Introduction to the Mechanical Properties of Ceramics*, Cambridge University Press, Cambridge, UK, 1998.
- S. Hayun, A. Weizmann, M.P. Dariel, N. Frage, Microstructural evolution during the infiltration of boron carbide with molten silicon, *Journal of the European Ceramic Society* 30 (2010) 1007–1014.
- P. Chhilar, M.K. Aghajanian, D.D. Marchant, R.A. Haber, M. Sennett, The effect of Si content on the properties of B_4C -SiC-Si composites, in: *Proceedings of the 31st International Conference on Advanced Ceramics and Composites, Advances in Ceramic Armor*

- III, Ceramic Engineering and Science Proceedings, 28 2007 pp. 161–168.
- [12] M.K. Aghajanian, Toughness enhanced silicon - containing composite bodies, and methods for making same, USP 6995103 B2 7(2006).
- [13] A.L. Yurkov, B.S. Skidan, A.B. Ponomarev, Reaction between boron carbide and silicon, *Ogneupory* 2 (1987) 31–33.
- [14] Z.F. Chen, Y.B. Su, Y.B. Cheng, Formation and sintering mechanisms of reaction bonded silicon carbide–boron carbide composites, *Key Engineering Materials* 352 (2007) 207–212.
- [15] A.L. Yurkov, A.M. Starchenko, B.S. Skidan, Reaction sintering of boron carbide, *Refractories and Industrial Ceramics* 30 (1989) 731–736.
- [16] M. Wilhelm, S. Werdenich, W. Wruss, Influence of resin content and compaction pressure on the mechanical properties of SiC-Si composites with sub-micron SiC microstructures, *Journal of the European Ceramic Society* 21 (2001) 981–990.
- [17] O.P. Chakrabarti, S. Ghosh, J. Mukherjee, Influence of grain size, free silicon content and temperature on the strength and toughness of reaction-bonded silicon carbide, *Ceramics International* 20 (1994) 283–286.
- [18] F. Thevenot, Boron carbide—a comprehensive review, *Journal of the European Ceramic Society* 6 (1990) 205–225.
- [19] P.G. Karandikar, G. Evans, S. Wong, M.K. Aghajanian, M. Sennett, A review of ceramics for armor applications, *Proceedings of the 32nd International Conference on Advanced Ceramics and Composites, Advances in Ceramic Armor IV*, Ceramic Engineering and Science Proceedings, 29 2008 pp. 163–175.
- [20] X.D. Yu, Y.W. Wang, F.C. Wang, Effect of particle size on mechanical properties of SiC_p/5210 Al metal matrix composite, *Transactions of Nonferrous Metallics Society of China* 17 (2007) s276–s279.
- [21] R.W. Hertzberg, *Deformation and Fracture Mechanics of Engineering Materials*, John Wiley & Sons, Inc., NY, USA, 1996.